POLITECNICO DI TORINO
Repository ISTITUZIONALE

Automotive VHDL-AMS Electro-mechanics Simulations

Original
Automotive VHDL-AMS Electro-mechanics Simulations / Graziano, Mariagrazia; RUO ROCH, Massimo - In: New trends and developments in automotive system engineering / M. Chiaberge (ed.). - ELETTRONICO. - Vienna : InTech, 2011. - ISBN 9789533075174. - pp. 541-566 [10.5772/13154]

Availability:
This version is available at: 11583/2375485 since:

Publisher:
InTech

Published
DOI:10.5772/13154

Terms of use:

This article is made available under terms and conditions as specified in the corresponding bibliographic description in the repository

Publisher copyright

(Article begins on next page)

23 April 2024

27

Automotive VHDL-AMS Electro-mechanics Simulations

Mariagrazia Graziano and Massimo Ruo Roch
Politecnico di Torino
Italy

1. Introduction

Automotive sub-systems, from security and energy, to comfort and entertainment, include several examples of entanglement between electronics and mechanics (H. Casier & Appeltans, 1998). Their correct modeling is of key importance during the design cycle, and, from conception to test, real critical conditions due to mechanic, thermal and electromagnetic stress sources must be taken into account. Typical design and test methodologies are both electronic and electro-thermo-mechanical, but they focus on a single fault source at a time. Moreover in most of the cases they are applied late in the design cycle. Accurately emulating a multi-disciplinary system during both design and test phases is of great importance when reliability is the first concern as in the automotive scenario case. The methodology tackled in this chapter, based on the VHDL-AMS language, can be applied both during design and performance or fault analysis and allows to focus on electronic devices internal parameters at a detailed level, and, meanwhile, to evaluate the influence of other electronics devices in the car system, the electro-mechanics of the vehicle and the static and dynamic usage conditions. One of the language/simulator used by system engineers in this field is Matlab/Simulink (Friedman, 2005) which allows modeling both electronic and mechanical systems at a very high hierarchical level, thus allowing to understand relations between the two fields from a system perspective. Problems arise when designers need to accurately model both electronic and mechanical devices.

VHDL-AMS (1076.1, 1999) is a superset of VHDL, thus not only digital constructs are supported but electrical quantities, differential equations and algebraic constraints can be modeled as well. The effect is the possibility to describe mixed-technology systems, ranging from mechanics to optics, from thermodynamics to chemistry without the need to change simulation tool. Its suitability for automotive electro-mechanical systems modeling results in the effectiveness in capturing the impacts of electronic blocks at the system level, and, on the other hand, in achieving a good understanding of impact mechanics on electronic design choices as well.

Multi-resolution is a further relevant VHDL-AMS characteristic: It allows to describe different blocks in the system using different levels of abstraction, depending on the focus needed for different devices. In the automotive context this is a great improvement as it implies, for example, that critical electronic blocks can be accurately described, while the thermo-mechanical car environment can be only approximately represented. This favours a lightweight simulation in terms of required CPU time. A further important achievement consists in the possibility to capture the effects of electronic details at the system level, and, on

the other hand, in obtaining a good understanding of mechanics impact on electronics design choices.
As a case of study on the subject, in this chapter we describe the behaviour of CD players for vehicle dashboard when realistic shocks through the vehicle suspension system due to the variable roadway profile are considered as environment conditions. A VHDL-AMS analysis environment is modeled based on the CD player electro-mechanical structure, on its connections to the vehicle dashboard, body, and suspension system, and on the relationships to roadway irregular profile. A real audio waveform is included in the simulation, modulated and transformed in the optical binary informations stored in the CD. Afterwords it is used as a real input.
This methodology is compared to traditional ones which imply real mechanical shocks transmitted to a CD player to emulate roadway profiles and audio quality detection.
We show that this multi-disciplinary and multi-resolution methodology, a new approach in fault-related literature, is feasible. We show that it allows to reproduce traditional shock tests as well. We thus demonstrate how faults conditions could be anticipated before the production phase. A simulation framework as the one described in this chapter gives the possibility to analyze the impact of electronics sub-systems parameters and of vehicle characteristics on system performance. This "integrated method" allows then to understand the failure sources connected to a real application environment and their possible solutions. This detailed information are not usually derived from traditional simulations and tests. In several points of the chapter, thus, evidences are given of how such a multi-disciplinary and multi-resolution methodology pinpoints that critical conditions could be anticipated before the production phase. On the author knowledge, often in the industrial field specific design values are not defined on a rigorous basis, but, on the contrary, chosen using a trial and error methodology. This is clearly expensive, especially in the car electro-mechanical system industry.
The chapter is organized as follows: in section 2 the principle of CD player electrical, mechanical and optical operations are given together with the vehicle suspension system organization, while in section 3 traditional test structures for autovehicle and dashboard CD player are described. In section 4 previous works based on VHDL-AMS are briefly reviewed and few hints on VHDL-AMS are reported. In section 5 the detailed model of the whole system is described giving VHDL-AMS examples, while in section 6 simulation results are presented and discussed. Final remarks and conclusions are in section 7.

2. The CD player in a car dashboard: electronic, optical and mechanical system

In this section the basic operations of the CD player (for details see Mansuripur (1994)) and the car system will be given without the aim of being exhaustive, as this is not the focus of the work.
Audio data, sampled at 44.1kHz, are not directly stored in the Compact Disk, but are partially modified to decrease error rates during music play back. Error codes insertion and interleaving are used during data packets creation. Furthermore, data are encoded using Eight Fourteen Modulation (EFM): Each 8 bits packet is encoded in a 14 bits one, in such a way that the number of '1's is as small as possible, and the distance between two '1's is as high as possible. Such encoded numbers are not directly stored on the CD support in the EFM form as each '1' is interpreted as a variation between a stored '0' (called *land*) and a stored '1' (called *pit*) or vice-versa. Thanks to EFM encoding, then, the physical distance between two transitions is higher than a given threshold. This is important as the reading system has an intrinsic

inertia and a limited accuracy in detecting the 0/1 or 1/0 variations. In figure 1 an example of data stored on the physical disk surface in terms of *pits* and *lands* and their correspondence to the EFM encoded data is shown. By means of a laser diode and a complex optical system

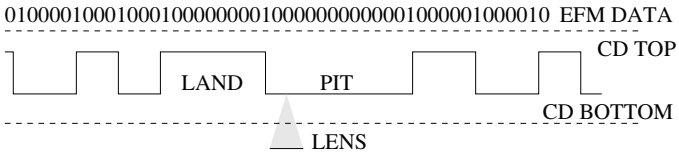

Fig. 1. CD pits and lands stored data.

a light signal with $\lambda \approx 500\,\text{nm}$ is focused on the bottom side of the CD. The light is reflected back by *pits* and *lands* with a phase difference. The *land* and *pit* vertical height is accurately sized so that the signal reflected by the land has a phase difference of 180° with respect to the incoming wave. Thus a destructive interference occurs and no light signal is noticed back at the detecting system – i.e. a *land* corresponds to a '0'. On the other hand, the *pit* fully reflects the signal, and thus it corresponds to a '1'. These informations are read back by the audio data reconstruction system. The pit/land sequence is stored in a spiral on the CD support. Each sequence is separated from its neighbour one by a *land* track, as detailed in figure 2. The

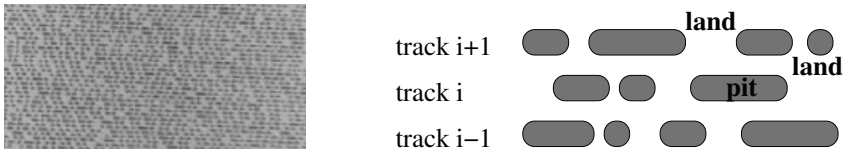

Fig. 2. CD data tracks. Left: photograph (Mansuripur, 1994). Right: detail of three tracks organized in pits and lands.

optical system, called *pick-up*, follows the track thanks to the rotation of the CD support due to a spindle motor and to a radial movement of the lens support. For a correct *pit/land* reading three important errors must be controlled. First, the optical system must be in focus; second, the laser should follow almost exactly the track spiral; third, the disk must be aligned to its ideal rotational axis. In the first case, shown in figure 3, if the lens is not at the right distance from the rotating disk, the focus point might not correspond to the *pit/land* surface, and the 0/1 data is incorrectly detected. The error is of vertical type and depends on external shaking, positioning tolerances or not planar CD surface. The tracking error, shown in the right sketch of figure 3, is of radial type, depends on bad disk centering and must be accurately checked as in a CD radius of about 3 cm the spiral may count up to 20000 adjacent tracks. Again, if this error is larger than a given threshold the 0/1 data is incorrectly detected. Last, due to the CD positioning system intrinsic errors, the disk may not be aligned to its ideal rotational axis: In this case both a vertical (focus) and a horizontal (tracking) error will be present. The CD player has an automatic system to control both focus and tracking errors. The signal reflected by the *pit/land* surface is elaborated by the lens system and deflected towards a photo-diode array. Whether the focus point is correct, then the deflection is uniform on all the photo-diodes; on the contrary, if the focus point is ahead of or behind the *pit/land* surface, each couple of photo-diodes senses a different deflected light. Uniform or different electrical signals will be then transmitted by the photo-diodes to an electronic system combining its inputs into a single amplified output correspondent to the detected focusing error. This signal will be used to drive a coil, which will generate the force needed to correct the optical system vertical

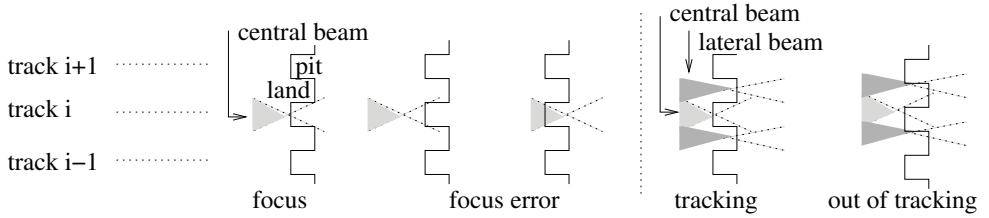

Fig. 3. Neighbour tracks stored in spirals as shown in figure 2. Focus and tracking errors.

position with respect to the disk. Theoretically, this feedback system will reach a balance point when the error is zeroed. In a real case, a given tolerance is the reached target. The tracking system is based on a similar principle and acts on the signal of other two photo-diodes. They receive, when on track, almost zeroed light back by the land spirals which are on the right and left of the main track spiral. These lands are lighted by two lateral components of the main laser diode emitted beam (details in figure 3 on the right). In case the radial motion of the lens system is not correctly following the track spiral, then the lateral components would reflect part of a pit of another track, and then the lateral diodes will receive a higher light signal. Consequent electrical signals at the two photo-diodes output are then combined to force a current on the coil responsible of the lens radial motion adjustment.
Both tracking and focus correction systems are influenced by external shaking, in particular in an auto-vehicle which is constantly moving on a not uniform surface. The most relevant accelerations are not the longitudinal or trasversal ones, which are usually negligible with respect to track system readings, but the vertical one, strongly influencing focus regulation.
Road irregularities are directly applied to car tyres, which transmit them to wheel axis, and to the moving part of the suspension system. The set built up by these three components is usually called *not suspended mass*, to underline its direct connection to the road, even if a little degree of displacement filtering is anyway guaranteed by tyres elasticity. The suspension system links the not suspended mass to the car body (called *suspended mass*), reducing the extent of vertical movement, thanks to the combined effect of its spring and shock absorber. The car body is then supposed to be connected to the dashboard, and to the CD player enclosure, with a structure of infinite stiffness, while the pick-up mass is linked to the CD player structure through a suitable damping system.
In section 5 details on the models used to describe the essential electronical, mechanical and optical systems are reported together with model approximations adopted in this work.

3. The traditional test equipment

Whenever dashboard CD player was tested by a specialized industry, a shaker system is adopted similar to the one used by our industrial partner (Magneti Marelli S.p.A.). In figure 4, a block diagram of a typical test configuration is shown. In the lower part a detailed view of the shaker actuator is visible, which propagates vibrations to the object fixed upon it according to a given vibrational profile. It is composed by three main blocks: an external fixed structure, an inductor, which is connected to it by means of a damper, and the vibrating plate upon which the object to be tested is fixed. The inductor is immersed in a static magnetic field, and, thanks to an appropriate current which flows through it, generates a force transmitted to the vibrating plate. The current is controlled by an external instrument connected to a PC and amplified before being injected in the inductor. Feedback through a control system is

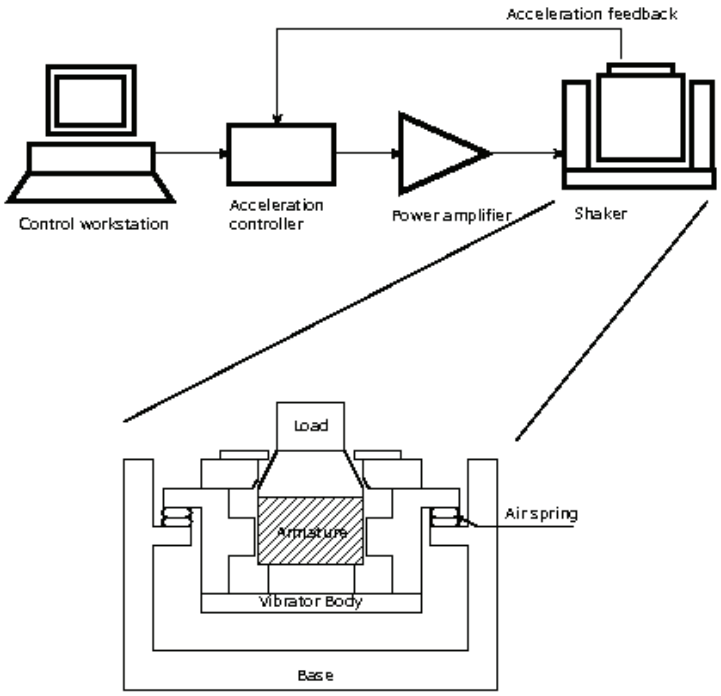

Fig. 4. Block diagram of CD player test configuration.

needed, to guarantee desired acceleration of the device under test. Input of the control system is the shaking profile defined by the user through the PC. This vibrating shape, in most of the cases, is directly provided by the CD player producer and should correspond to the maximum shocks tolerated by the device. The most frequently used profiles are of *sine* and *bump* type. In the former case, frequencies are automatically swept within a range chosen by the user. The aim is to analyze the response when a continuous vibration is present, as, for example, in the case of an auto-vehicle driving on a constantly irregular road profile. In the latter wave, a single but more violent vibration is used to test the CD player functionality (often, a sine semi-period is used as a profile) emulating a unique road irregularity.

The problems with this kind of tests are threefold. First, the vibrational profiles should be as similar as possible to the dashboard ones, but, on one hand, they are extremely dependent on the vehicle characteristics, and, on the other hand, the shaker system, even if carefully controlled, may introduce differences with respect to a real car system. Second, CD player performance are revealed by listening to the audio track and simply defining if, and how much frequently, an interruption occurred. Even if near to what the car user perceives, this is only a superficial error detection, it is subject to the user who is executing the test, and, most important, is an on-off test, as it does not reveal the error entity nor the location of the cause. Third, these are performed very late in the production cycle, as they are post-production tests or, in many cases, executed once the car producer has already installed the player and verified a systematic failure in the car plus CD player ensemble. From the point of view of CD player

or car manufacturers the information available after the execution of this kind of tests are far from being useful. In fact the need is to understand how and in which point modifications suitable to problem recovery can be performed. Moreover, the kind of vehicle must be taken in account as well. Even if this traditional system can still be useful, new, more sophisticated methods should be adopted to avoid long and expensive trial-and-error iterations.

4. VHDL-AMS: a multidisciplinary language for multi-resolution simulations

The VHDL language is thought for discrete systems modeling, like digital signals in digital circuits, but nowadays designs often needs the description of continuous characteristics. For example this happens in digital systems when sub-micron effects must be taken into account, or in analog and mixed-signal electrical design, or even in mixed electrical/not-electrical systems. VHDL-AMS supports discrete features but allows the adoption of continuous models based on differential algebraic equations, thanks to a dedicated analog solver. A few works document the use of VHDL-AMS as an effective simulation language for efficient design of complex mixed-signal electronics systems (Christen & Bakalar, 1999), especially in the telecommunication field. In (R. Ahola & Sida, 2003) a Bluetooth transceiver was first modeled using a simple behavioral description. Later, few blocks where refined and described so as to match the transistor level model. Basic functionality tests using an abstract VHDL-AMS behavioural description were used in (J. Oudinot & Le-clerc, 2003) showing the feasibility of a full transceiver circuit simulation. In (E. Normark & Nikitin, n.d.) RF blocks of a DQPSK transceiver and a channel model were implemented adding white Gaussian noise and achieving results very close to theoretical models. A methodology for the design of RF circuits in VHDL-AMS starting from flexible specifications and assuring an accurate description of noise and nonlinear effects was proposed in (W. Yang & Yan, 2005). In (Godambe & Shi, 1998) the real behavior of a PLL was modeled using VHDL-AMS adding jitter: the phase noise simulated spectrum was in good agreement with measured results. A top-down design methodology, validated by measurements, was proposed in (V. Nguyen & Naviner, 2005) for the design of a delta-sigma modulator. After a coarse description of components, various error sources like jitter, thermal noise, and capacitor mismatch were added to models. The modulator was finally designed in a CMOS process and measurements confirmed both model accuracy and top-down methodology effectiveness. In (L.A.Barragan & Burdio, 2008) authors use both VHDL and VHDL-AMS to model digital and mixed-signal circuits thought to reduce conducted electromagnetic interference (EMI) caused by resonant inverters in induction heating home appliances. A methodology for the design, the simulation and the fault analysis of a Controller Area Network (CAN) bus is presented in (W. Prodanov & Buzas, 2009). In (Santarini, 2006) VHDL-AMS is suggested to model complex electronic systems interacting inside the automotive environment, with varying hierarchical depth. An interesting application to automotive systems is in (M. Gursoy & Pelz, 2008) where a methodology is presented to investigate and predict the effects of the interaction between CAN transceivers and twisted pair transmission line connecting them in terms of electromagnetic emission. The language ability to solve differential algebraic equations allows modeling of not-electronic systems. In (F. Pecheux & A.Vachoux, 2005) several disciplines are involved in the modeling of an airbag system. Electrical, thermal, optical, mechanical and chemical knowledges are synthesized in the resulting model. A further up-to-date example is in F. Gao & Moudni (2010), where a multidomain dynamic proton-exchange-membrane fuel-cell stack model is described and simulated using VHDL-AMS. In (H. Boussetta & Soudani, 2010) a physical model of a microelectromechanical system piezoelectric microgenerator and its controlling

circuit is presented and their interaction analyzed. This capability is in fact particularly suitable to accurately represent automotive electro-mechanic components. Actually, the design of automotive systems requires a multitude of single components and sub-blocks, while, at the same time, complete system analyses are needed as well. In (Moser & Mittwollen, 1998) the first results of a joint project between automotive industry partners and tool makers are presented in the modeling of a brake system with ABS including hydraulics, mechanics and control aspects. In (D. Metzner & Schafer, 2002) a methodology for VHDL-AMS based specification, design and verification of an automotive Smart Power IC is presented. In (Wang & Kazmierski, 2005a) the same language is used for modeling, simulating and optimizing a fuzzy logic controller for an active suspension system. In (Wang & Kazmierski, 2005b) mixed mode simulation is the basis to model an active vibration isolation system in automotive environment. As previously pointed out, the VHDL-AMS language has another key characteristic: it allows to describe systems with different levels of abstraction. This makes a top-down design methodology viable, in which a preliminary behavioural description of components allows a coarse functionality test of the system, while progressive refinements define real circuit performance. This feature is particularly enhanced by ADMS (MentorGraphics, 2004) which allows to co-simulate both high level VHDL-AMS architectures and Spice-level netlists using ELDO in the same simulation environment, as shown in (M. R. Casu & Zamboni, 2007)(M.R. Casu & Graziano, 2008). In case an automotive device was to be modeled, this multi-resolution capability implies that critical electronic blocks can be roughly described at first. Later they are accurately refined, thus exploiting the native VHDL-AMS strength in modeling digital and analog devices, if needed, down to transistor level. On the other hand, the thermo-mechanical car environment can be coarsely represented, if less important, thus allowing a lightweight simulation from the point of view of CPU time. It is then of great interest the possibility to capture the effects of electronic details at system automotive level, and, conversely, the crucial capability of deriving electronic device design constraints from car system bound required performance. The design of the electronic system will be thus effectively optimized taking into account a real mechanical environment, so that reliability and fault test cases are reduced. In this work, starting from (Bisoffi, 2006) even if we do not go into details of the electronic system, we show how it is possible to create, early in the production phase, a fault analysis exploiting VHDL-AMS capabilities. It means co-simulating electronic and mechanical devices to point out their entangled operations, and, most important, analyzing how the performance of such a system is influenced by its real application environment.

5. Modeling dashboard CD player using VHDL-AMS

In section 5.1 we will describe the entire car and CD player macro-blocks and their principal interactions, while in the successive sections we will focus on the most important sub-blocks.

5.1 The system

The block diagram described using VHDL-AMS is shown in figure 5, in which the three mechanical, electrical and optical systems are depicted, together with their relationships.
The *mechanical* block includes the car tyres and suspensions system, the dashboard, the CD external structure, the pick-up and the track control sections. Inputs of this part are:

- Anterior and posterior roadway profiles to the tyres **Z-road-ant** and **Z-road-post**.
- **Vertical shift** and **radial shift** of the disk due to an error in its positioning system.

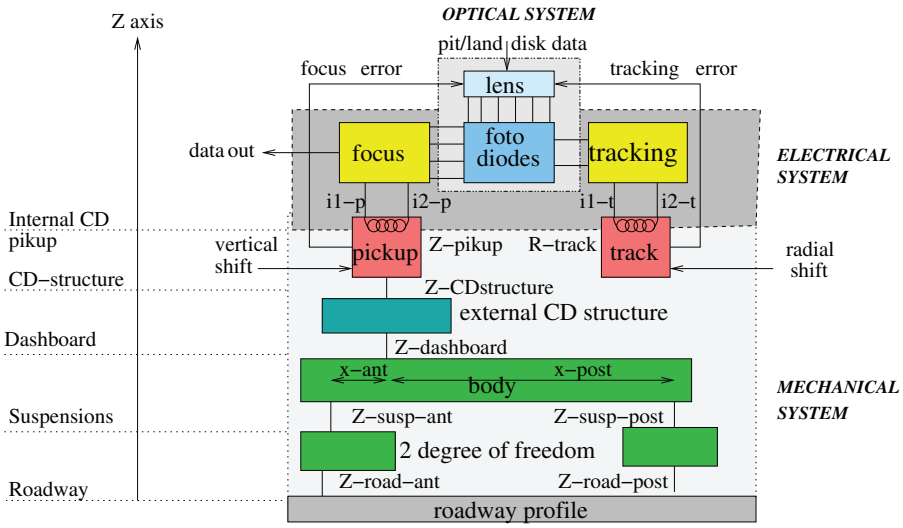

Fig. 5. Block diagram of the car and CD player mechanical (dotted box), electrical (dashed box) and optical (dash-dotted box) systems.

- Inductors currents of the pick-up **i1-p, i2-p** and radial tracking **i1-t, i2-t**, driven by the electrical system.

The pick-up and track block positions **Z-pickup** (vertical) and **R-track** (radial) are the physical outputs, used in the model to generate the **focus** and **tracking** error, used as inputs of the optical system model.
State variables are the vertical positions of the suspensions, the dashboard and the CD structure. Parameters are the auto-vehicle and CD player mechanical characteristics.
The *electrical* block includes the focus and tracking control devices and the audio data reconstruction system. Photo-diodes output signals **a, b, c, d, e, f** are the inputs, while the currents for the pick-up and tracking coils (**i1-p, i2-p**, **i1-t, i2-t**) and the binary **data out** correspondent to *pit* and *land* variations are the computed outputs. The electrical characteristics of electronic control devices are the parameters of this system.
The *optical* block is composed of lens and photo-diodes. It receives as inputs **pit/land** physical track data and **focus** and **tracking** errors from the mechanical system. Last, it generates as outputs the photo-diodes signals. The latter devices characteristics are parameters for this system, together with the factors we used to model optical lenses.

5.2 The car model

We simplified the model assuming the vehicle was symmetrical with respect to the longitudinal axis. Moreover, the suspension system is simplified, as already explained in section 2 using a two degrees of freedom (*2dof*) De Carbon model of type mass-spring-damper, representing one quarter of the vehicle and sketched in figure 6. The model consists of two masses, the suspended (*Ms*) and the not-suspended (*Mns*) ones. The former includes vehicle structure and half of the spring-damper-suspension mass. The latter includes wheel and its connection structure, brake and the other half of above-mentioned mass. Both suspension and tyre are modeled with their rigidity and damping factors *Ks*, *Cs*, *Kt*, *Ct*.

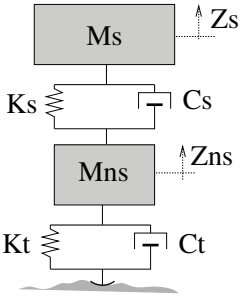

Fig. 6. Mechanical model of two degrees of freedom car suspension.

The depicted model leads to the following differential equations pair:

$$\frac{d^2Z_s}{dt^2} = \frac{K_s(Z_{ns}-Z_s)+C_s(\frac{dZ_{ns}}{dt}-\frac{dZ_s}{dt})}{M_s}$$

$$\frac{d^2Z_{ns}}{dt^2} = \frac{K_t(h-Z_{ns})+C_t(\frac{dh}{dt}-\frac{dZ_{ns}}{dt})-M_s\frac{d^2Z_{ns}}{dt}}{M_{ns}}$$

According to them, the resulting VHDL-AMS description of the two degrees of freedom system can be written in the following way:

```
entity twodof is
  generic (constant Kt :REAL := 0.0;
           constant Ct :REAL := 0.0;
           constant Ks :REAL := 0.0;
           constant Cs :REAL := 0.0;
           constant Mns :REAL := 0.0;
           constant Ms: REAL := 0.0);
  port (terminal t_h,t_zns,t_zs: translational);
end entity twodof;

architecture Level0 of twodof is
  quantity h across t_h to translational_ref;
  quantity zns across zns2 through t_zns
                        to translational_ref;
  quantity zs across zs2 through t_zs
                        to translational_ref;
  begin
    zs'dot'dot == (Ks*(zns-zs) +
                  + Cs*(zns'dot-zs'dot))/Ms;
    zns'dot'dot == (Kt*(h-zns) +
                  + Ct*(h'dot-zns'dot) +
                  - Ms*zs'dot'dot)/Mns;
end architecture Level0;
```

The structure is composed, as in standard VHDL, by an **entity**, *twodof*. Rigidity and damping parameters are passed as **generic**s, which values are set when this block will be instantiated within the higher hierarchical levels of the architecture. The **ports**, instead, represent the available connections to other blocks.

They are of *translational* type, an addition in the VHDL-AMS syntax with respect to traditional VHDL. They represent as *translational_ref* the position (t_h, that is, the road), the not-suspended mass position (t_{zns}) and, the suspended mass position (t_{zs}), respectively.

The model is described in the **architecture** part, in which two differential equations allow to find the position of the two masses with respect to the road profile. For describing the equations system VHDL-AMS uses the variable called **quantity**, which can be of the needed physical type, in this case *translational*. Each quantity is based on **through** and **across** variables that can be assimilated to a current and a voltage in an electrical system. An example is in figure 7, where through and across variables are shown for an electrical, a mechanical and a thermal system.

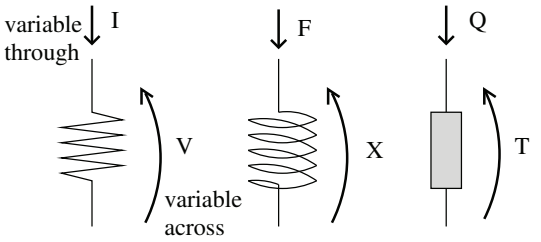

Fig. 7. Electrical, mechanical and thermal VHDL-AMS through and across variables.

A reference model, based on Matlab-Simulink blocks, and shown in figure 8, has been realized as well, to compare description complexity and results reliability with respect to more standard modeling techniques. As can be easily seen, VHDL-AMS allows to use a simpler description, leading to easier model understanding and maintenance.
Simulations have been performed, then, to compare system behaviour with the two modeling techniques, excited by manifold road profiles. As an example of the obtained results, in figure 9 the suspension position (Z_s) caused by a typical bump on the road is reported for the two models. The profiles are almost superposed, thus showing a good reliability of the VHDL-AMS description. The input is exactly one half period of sine wave with 10 cm amplitude and 10 Hz frequency.
The vehicle described in our model is composed of two *2dof* blocks connected to the front and back axles, as sketched in figure 5. They are used to reckon the dashboard vertical position using the vehicle body model and the distances between the dashboard and the two suspensions ($x - ant$ and $x - post$). For simplicity, in our model, car body is supposed to be rigid, and dashboard position is computed as

$$Z_{dashboard} = \frac{Z_{susp-ant}x_{ant} + Z_{susp-post}x_{post}}{x_{ant} + x_{post}}$$

This complexity reduction leads to four degrees of freedom compared to eight ones and will collapse the influence of the road irregularity on the vertical error. We will not take into account radial error effects due to different road profiles coupled to two tyres on the same axle. This does not influence essential results of our work, but will be implemented in its future development to improve results accuracy. Suspension parameter values used in our simulations are for two kind of vehicles: a comfort one and a handling one, representing two different kind of performance required by suspension systems. Their values are reported in table 1.
The car system *vehicle* is described using VHDL-AMS stepping up to a higher hierarchical level, which includes the body model and the suspension block as components, as reported in the preceding code. Before the real architecture description begins, four terminals are declared for supporting the connections among the blocks. The architecture is described using one instance of the body (*vehicle-instance*) and two instances (front and back) of the *2dof* blocks (*anterior-susp-instance* and *posterior-susp-instance*).

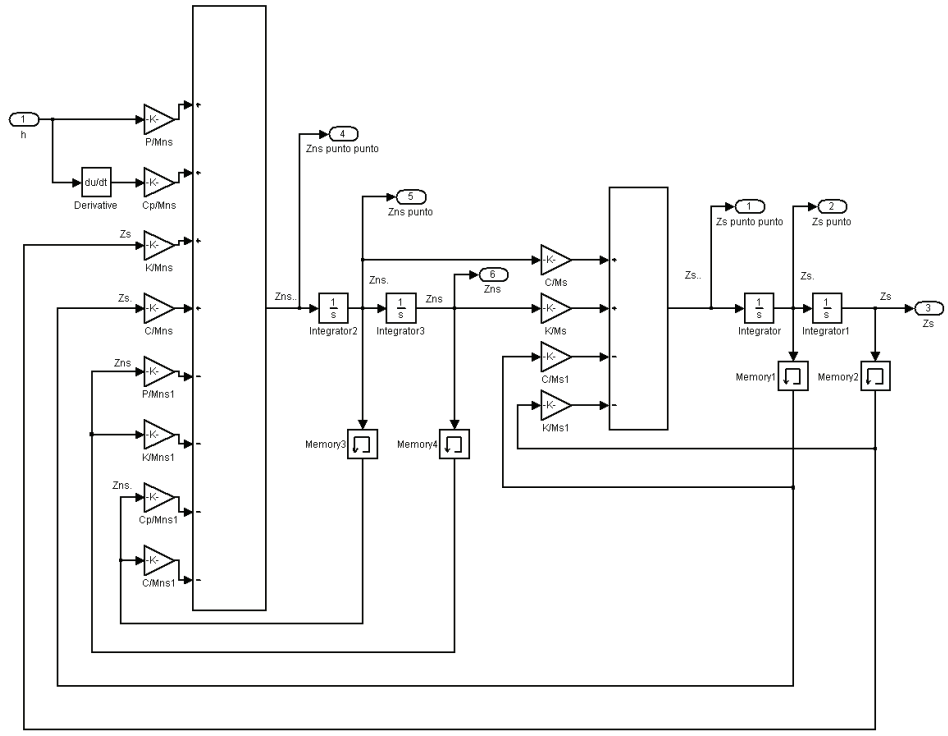

Fig. 8. Matlab-Simulink model of two degrees of freedom car suspension..

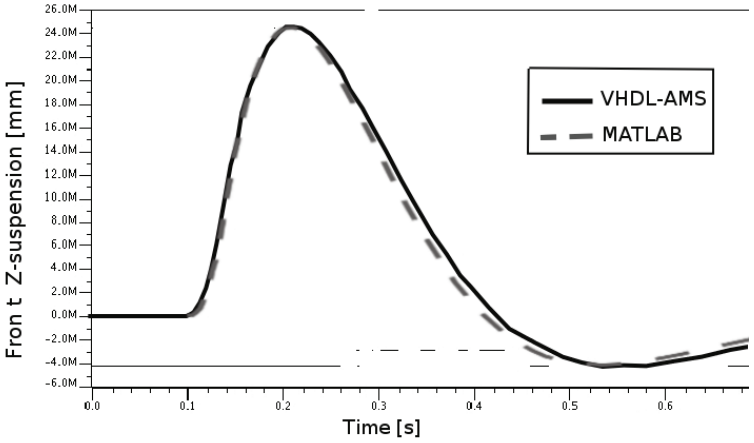

Fig. 9. Suspension displacement (Z_s) for a roadway bump profile. Matlab and VHDL-AMS simulation results.

	Comfort		Handling	
	front axle	**back axle**	**front axle**	**back axle**
m_s	756.7 Kg	596.3 Kg	756.7 Kg	596.3 Kg
m_{ns}	85 Kg	80 Kg	85 Kg	80 Kg
Ks	33333.3 N/m	21428.6 N/m	46666.6 N/m	30000.04 N/m
Cs	8667 N/(m/s)	6667 N/(m/s)	12133 N/(m/s)	9333 N/(m/s)
Kt	17000 N/m	17000 N/m	+40 23800 N/m	23800 N/m
Ct	1000 N/(m/s)	1000 N/(m/s)	1400 N/(m/s)	1400 N/(m/s)

Table 1. Rigidity and damping factors for comfort and handling vehicle models.

```
entity vehicle is
  port (terminal t-road-ant, t-road-post,
        t_dashboard: translational);
end veicolo;

architecture Level1 of vehicle is
 component twodof
   generic ( constant Kt :REAL := 0.0;
             constant Ct :REAL := 0.0;
             constant Ks :REAL := 0.0;
             constant Cs :REAL := 0.0;
             constant Mns :REAL := 0.0;
             constant Ms: REAL := 0.0);
   port (terminal t_h, t_zns,
                  t_zs: translational);
 end component;
 component bodymodel
   generic (constant x-ant :REAL := 0.0;
            constant x-post :REAL := 0.0);
   port (terminal t_zsant, t_zspost,
                  t_zdash: translational);
 end component;

 terminal zns_ant, zns_post,
          zs_ant, zs_post: translational;
begin
  vehicle-instance : bodymodel
  generic map (x-ant => 0.82, x-post => 1.88)
  port map ( t_zsant => zs_ant, t_zspost =>
             zs_post, t_zdash => t_zdashboard);

  anterior-susp-instance : twodof
  generic map ( Kt => 1.7e5, Ct =>1.0e3,
                Ks => 33333.3, Cs => 8666.6,
                Mns => 85.0, Ms => 756.7)
  port map ( t_h => t-road-ant, t_zns =>
             zns_ant, t_zs => zs_ant);

  posterior-susp-instance : twodof
  generic map (Kt => 1.7e5, Ct =>1.0e3,
               Ks => 21428.6, Cs => 6666.6,
               Mns => 80.0, Ms => 596.3)
  port map ( t_h => t-road-post, t_zns =>
             zns_post, t_zs => zs_post);
end Level1;
```

Their terminals are properly connected by a **port map** and **generics** are set to values correspondent to the vehicle model (see table 1). The top level block is connected to the road profile. This is described, by means of mathematical expressions, as a vertical translation of the two terminals describing the *Z-road-ant* and *Z-road-post* positions. Three different profiles have been adopted: a *sine* wave, a *bump* (a sine semi-period) and a *step*, in all cases with parametric amplitudes and frequencies.

5.3 The CD mechanical structure

The block connected to the car body/dashboard is the CD external structure. It has the *Z-cdstructure* vertical position. We suppose a rigid connection between the two masses as usually no suspension system is used by automotive or CD player manufacturers. The optical body, which position is *Z-cd*, is linked to the CD external structure, thanks to a suspension system which limits vibrations transmission from the dashboard to the pick-up. Rigidity and damping factors which model such suspension are shown in figure 10. The CD pick-up must be kept at right distance from the CD surface, so that tracks are correctly beamed. To accomplish this, a coil corrects the pick-up position (*Z-pickup*) thanks to a current signal *i* imposed by the focus block through terminals *i1-p, i2-p*. The block diagram shows the force generated by the coil, the inertia opposed by the pick-up mass, and the rigidity and damping factors of the spring connecting the two components.

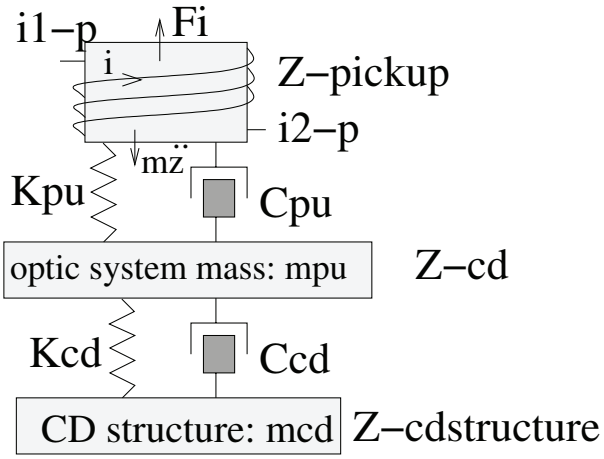

Fig. 10. Mechanical model of the CD structure.

The CD pick-up VHDL-AMS code is reported in the following. Two mechanical and electrical descriptions can be easily recognized. The rigidity and dumping parameters, together with the *Ki* constant in the permanent magnet law, are extremely important for CD behaviour and performance. The values adopted are reported in table 2. They have been obtained from CD player specifications, when available, and through a parametric study of the CD behaviour compared with traditional test results.

```
entity pickup is
  generic (constant Ki : REAL := 0.0;
           constant Cpu  : REAL := 0.0;
           constant Kpu  : REAL := 0.0;
           constant mpu: REAL := 0.0;
```

```
          ind :inductance := 0.0;
          i_ic : real := real'low);
  port (terminal t_zstrcd, t_zpu: translational;
        terminal i1-p, i2-p: electrical);
end entity pickup;

architecture Level0 of pickup is
  quantity h across t_zstrcd to translational_ref;
  quantity z across z2 through t_zpu
                              to translational_ref;
  quantity v across i through i2-p to i1-p;
  quantity Fi: force;
 begin
  if domain = quiescent_domain and
      i_ic /= real'low use i == i_ic;
  else v == ind * i'dot;  end use;
  z'dot'dot == (Kpu*(h-z) +
               + Cpu*(h'dot-z'dot)-Fi)/mpu;
  Fi == Ki*i*(z+1.0-h)**2;
end architecture Level0;
```

The tracking system is similar to the focus one, but simpler. It has no connection to the dashboard: only a system similar to the pick-up one reported in the previous VHDL-AMS code. As described above, CD position may be subject to variation with respect to the ideal one: This corresponds to vertical and radial shifts. These errors are here modeled as displacements forced by the external world. Both the focus and tracking mechanical sub-blocks, thus, have been modified by adding as inputs the **vertical shifts** and **radial shifts** respectively. Again, the updated model is not included for sake of brevity.

Kcd	**Ccd**	**Cpu**
$3.0e^4\,N/m$	$3.0e^4\,N/(m/s)$	$10\,N/(m/s)$
Kpu	**Ki**	**mcd / mpu**
$100\,N/m$	$35\,N/Am^2$	$0.5Kg/0.02Kg$

Table 2. Values adopted for the CD pick-up model.

5.4 The focus and tracking electrical subsystems

The focus block elaborates photo-diodes currents to accomplish the following tasks:

- First, it decides if a '0' or a '1' is present in the CD track.
- Second, it generates an error signal to correct the pick-up position if the four signals from the photo-diodes **a, b, c, d** are different, i.e., the CD surface is out of focus.

Focusing block architecture is reported in figure 11. Four amplifiers buffer impedances of the photo-diodes output to the cascaded block. A differential amplifier generates then the signal

$$Vd = \frac{R}{R_{abcs}}(b+d) - (a+c)$$

(if $R_a = R_b = R_c = R_d = R_{abcs}$) related to the photo-diodes physical position and the optical deflection system. As reported in above boxes in figure 11, when the pick-up is in the right position all photo-diodes receive the same signal, thus $Vd = 0$. Otherwise, depending on the focus point position, ahead of the track line or behind, the photodiodes receive vertically or horizontally unbalanced light signals respectively. The differential signal Vd will be thus negative or positive. An example of the VHDL-AMS code used to behaviourally model the operational amplifier is in the following.

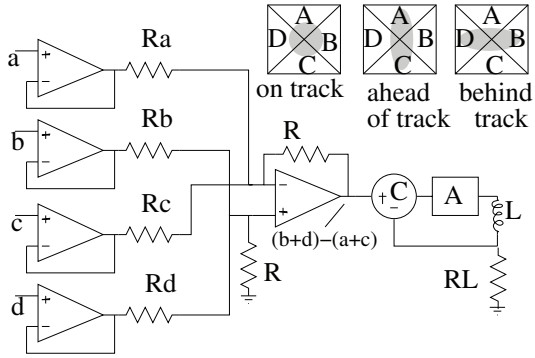

Fig. 11. Focus electrical subsystem.

```
entity opamp is
  generic (alim_plus : REAL := 12.0;
           alim_min : REAL := -12.0;
           gain : REAL := 1.0e5);
  port (terminal in_plus, in_min,
                 out_op: electrical);
end opamp;

architecture Level0 of opamp is
   quantity vd across in_plus to in_min;
   quantity vout across i_out through out_op
                              to electrical_ref;
   quantity q : REAL;
 begin
        q == vd*gain;
        if q > (alim_plus-0.5) use
          vout == alim_plus-0.5;
        elsif q < (alim_min+0.5) use
          vout == alim_min+0.5;
        else
          vout == q;
        end use;
end architecture Level0;
```

In this work we did not model any amplifier offset error as they are considered not meaningful with respect to the impact of mechanical induced vibrations on system performance. On the other hand, we model saturation effects in our description, as such distortion could affect focusing block effectiveness. Anyway, it will be interesting to include in future developments of this work second order effects of electronic devices as well, in order to asses their impact on focusing error. The V_d signal should be able to drive the coil which generates the force needed to correct the pick-up position, as described in section 5.3. This is realized by a system with feedback that generates a bipolar current needed to drive the linear motor coil L. VHDL-AMS code of this circuit is not reported for space reasons. The tracking block has a similar structure and acts on two other photo-diode outputs (**e** and **f**) generating a zero signal when the system is on track: If a lateral shift occurs on the laser direction with respect to the track, the light received by the two photo-diodes is unbalanced. The correction occurs again forcing a current with proper direction and amplitude on the tracking block coil.

5.5 The optical subsystem

The optical block includes a photo-diodes array and the lens part. The VHDL-AMS behavioral model of one of the photo-diodes is reported below. The light intensity is defined as an *electrical* quantity for simplicity.

```
entity photodiode is
  port (terminal A, C, E: Electrical);
end photodiode;

architecture Level0 of photodiode is
   quantity v across i through A to C;
   quantity lum across E to electrical_ref;
 begin
    i == -8.2e-6*lum;
end Level0;
```

The light terminal is connected to the lens block, which code is reported in the following. This has been modeled in a simple way, as it is normally a closed-box which, in its internal composition, is not influenced by the errors we are considering. The emitted light focus point is influenced by the position of the optical block. For this reason, outputs for this entity are the emitted light signal of the six diodes **Eea, Ee, Eec, Eed, Eee, Eef**. Inputs of this entity are **sign_foc** and **sign_track**, that is the *pit/land* nominal input transition sequence and the track-ok land signal respectively. In much detail, it must be underlined that the real light signal reflected back by the track is not an abrupt one, but, still modulated, has a shape similar to the one reported in figure 12. We generated it (for details see Mansuripur (1994)) starting from the digital EFM data as described in section 6.

```
entity lens is
 generic (constant toll_foc :REAL := 0.0;
  constant toll_track :REAL := 0.0;
  constant K_foc :REAL := 0.0;
  constant K_track: REAL := 0.0);
 port (terminal in_err_foc,in_err_track: translational;
  terminal Eea,Eeb,Eec,Eed,Eee,Eef: electrical;
  terminal sign_foc, sign_track: electrical);
end entity lens;

architecture Level0 of lens is
 quantity err_foc across in_err_foc
          to translational_ref;
 quantity err_track across in_err_track
          to translational_ref;
 quantity sig across sign_foc to electrical_ref;
 quantity land across sign_track to electrical_ref;
 quantity Qeea across iea through Eea to electrical_ref;
 quantity Qeeb across ieb through Eeb to electrical_ref;
 quantity Qeec across iec through Eec to electrical_ref;
 quantity Qeed across ied through Eed to electrical_ref;
 quantity Qeee across iee through Eee to electrical_ref;
 quantity Qeef across ief through Eef to electrical_ref;
 quantity verify_foc: voltage;
 quantity verify_tracking: voltage;
 begin
  if err_foc'ABOVE(toll_foc)  use
      Qeea == sig ;  Qeec == sig ;
   if sig'ABOVE(K_foc*(err_foc-toll_foc)) use
```

```
      Qeeb == sig-K_foc*(err_foc-toll_foc);
      Qeed == sig-K_foc*(err_foc-toll_foc);
    else
      Qeeb == 0.0;   Qeed == 0.0;
    end use;
   elsif err_foc'ABOVE(-toll_foc) use
      Qeea == sig;   Qeeb == sig;
      Qeec == sig;   Qeed == sig;
    else
      Qeeb == sig ;  Qeed == sig ;
     if sig'ABOVE(-K_foc*(err_foc+toll_foc)) use
      Qeea == sig+K_foc*(err_foc+toll_foc);
      Qeec == sig+K_foc*(err_foc+toll_foc);
     else
      Qeea == 0.0;   Qeec == 0.0;
    end use;
    end use;
    verify_foc == Qeea+Qeec-Qeeb-Qeed;

    if err_track'ABOVE(toll_track)  use
      Qeef == land;
    if land'ABOVE(+K_track*(err_track-toll_track)) use
      Qeee == land-K_track*(err_track-toll_track);
    else
      Qeee == 0.0;
    end use;
   elsif err_track'ABOVE(-toll_track) use
      Qeee == land;   Qeef == land;
   else
      Qeee == land;
    if land'ABOVE(-K_track*(err_track+toll_track)) use
      Qeef == land+K_track*(err_track+toll_track);
    else
      Qeef == 0.0;
    end use;
   end use;
   verify_tracking == Qeef-Qeee;
end architecture Level0;
```

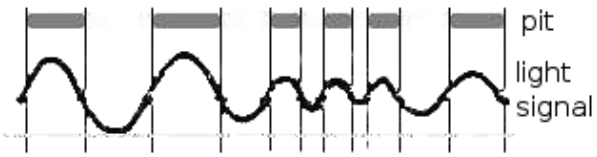

Fig. 12. Example of the EFM modulated light signal received by the photo-diodes when the track reflects back the laser light.

Further inputs of this block are position errors generated by the focusing and tracking systems described in section 5.3: **in_err_foc** and **in_err_track**. In absence of focusing error, light signals are identical to the **sign_foc** input. If a focusing error is occurring, light waves are unbalanced towards the correspondent diodes, as described in section 5.4, depending on error sign and on the value of a proper constant **K_foc**. In the same way the **Eee, Eef** signals depend on tracking error and the constant **K_track**. Tolerance factors are defined for both focus and tracking errors.

6. Simulation results

Every single block has been separately simulated and its behavior compared, when feasible, to the one found in the laboratory in collaboration with our industrial partner. System simulations consist in forcing irregular road profiles, of bump type or of sine type, in analyzing the focusing and tracking errors, when a digital data is forced at the CD input, and in comparing digital input and output. These data have been generated starting from a "wav" file, transformed in a EFM modulated input, and then digitized so that a '1' corresponds to a 'pit' in the CD track and a '0' corresponds to a 'land'. Afterwards these *pit/land* data are transformed in a light signal as in figure 12 and used as input to the *lens* block described in section 5.5. Road profile inputs reproduce the ones used in the traditional test described in section 3 (e.g. sin, bump, step). Several simulations have been accomplished varying available stimulus parameters. The main values used are wave shape (bump and sine are reported here), wave maximum amplitude (10cm and 20cm are reported herein), bump duration and stimulus frequency. Moreover, presence or absence of a CD rotational axis displacement and, finally, the vehicle type (comfort and handling) have been varied. Digital output generated by the pick-up system is compared with the input: When different, the fault simulation engine points out a logical error, as sketched in the simulation output in figure 13. In all illustrations of this section, N and M letters on axis are scaling factors, representing 10^{-9} and 10^{-3}, respectively.

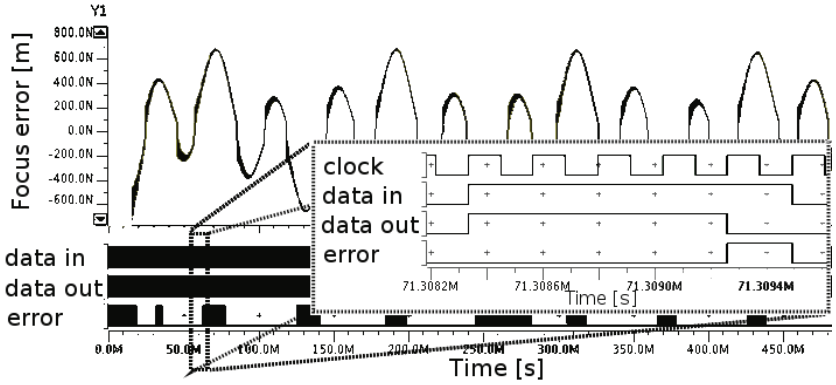

Fig. 13. Digital input, focus error, digital output and digital error.

Traditional test results are available only as presence or absence of audible audio errors. Our comparisons demonstrates that the detection of an error in the simulation is a needed but not sufficient condition to have an audible error in the real system. This behaviour can be ascribed to the following factors:

a) Error detection in the real system is accomplished through human ear, thus allowing to skip subtle glitches.

b) Our model does not take in account the ECC performed by electronic circuitry down the reproduction chain.

From this point of view, our test is more reliable as it is deterministic and does not depend on subjective chacteristics. Anyway, as our simulation environment allows to go deep inside data error sources, we prefer to analyze and report in the following focusing error behaviour dependency on the parameters. We will concentrate only on focusing error and neglect the

tracking one, as less dependent on the car system in our simple four degrees of freedom model. A focusing error greater than 0.5 μm is considered a critical one as, for sure, it causes a 0/1 evaluation error. A near to 0.5 μm error is still critical, but may not generate a digital error: This depends on the optical and electrical device parameters. We will then analyze the cases in which this error approaches the critical range. In figure 14 the case of a bump wave (10cm maximum amplitude) is reported, with a disk perfectly aligned to its rotational axis

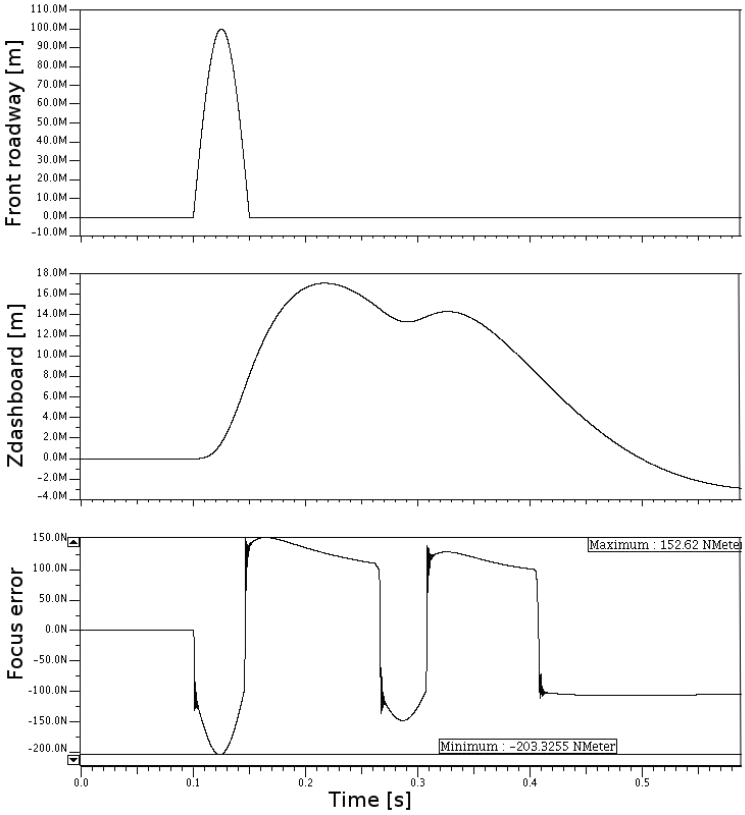

Fig. 14. Dashboard displacement and focus error in case of a bump road profile for a comfort vehicle suspension. No disk radial or vertical shift are used.

(radial and vertical shifts are zero, that is, an unrealistic state). The dashboard displacement is sketched as well, showing the superposed effects of the front and back axles. The focus error approaches a maximum of 200nm, which, at least in our simple model, is not expected to cause a digital error. In figure 15 the same signals are reported in case of a sine wave. The error is clearly dependent on the sine frequency and reaches higher values: The continuous roadway irregularity impacts on the focus correction system which is less capable to react to perturbations.

Figure 16 shows again a bump waveform as roadway profile, but a CD vertical shift is present as well, modeled as a sine wave of 1mm peak and 8Hz frequency. Both the suspension and the dashboard displacements are presented: Two different waves are superimposed for the

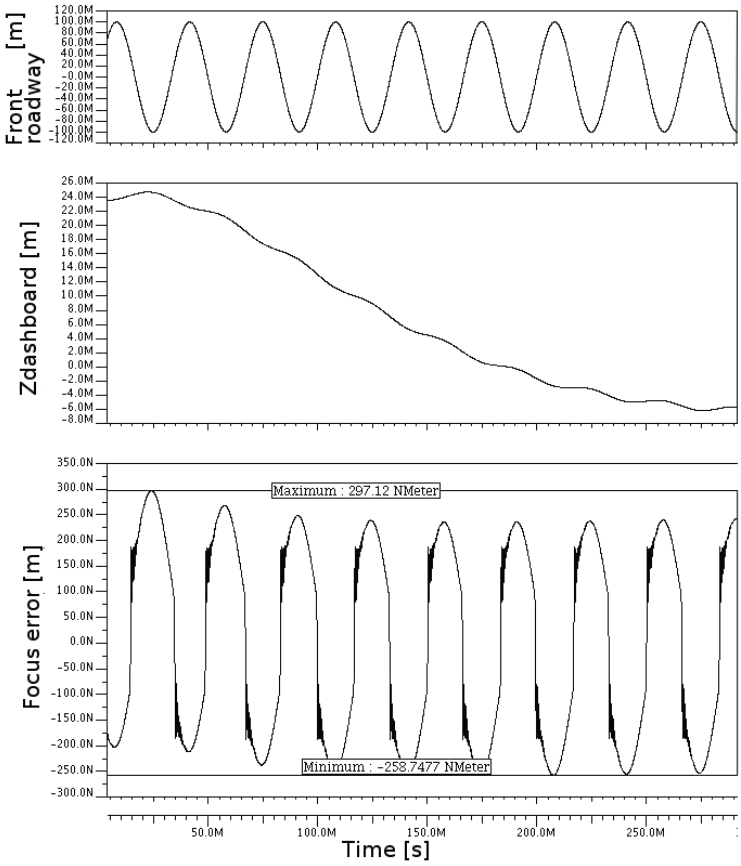

Fig. 15. Dashboard displacement and focus error in case of a sine road profile for a comfort vehicle suspension. No disk radial or vertical shift are used.

suspension parameters of a comfort and a handling vehicle respectively. The comfort model exhibits an almost doubled focus error if compared to the absence of the disk irregular rotation axis. The handling vehicle shows a 40% displacement increase with respect to the comfort one, with a 10% focus error increase. It is interesting to analyze the focus error data in table 3 in which the bump profile results are summarized. The bump peaks used were 0.1m and 0.2m long, and three bump durations are considered – correspondent to three different road irregularity lengths (ΔT).

A double bump amplitude has, of course, a higher impact on focus error when the CD is ideally rotating, while, the more realistic case of a periodical vertical shift causes only a 12% focus error worsening.

In figure 17 a simulation is reported in case of a sine road profile (0.1m peak, 25Hz) with a CD vertical shift for both a comfort and a handling vehicle. In this case the focus error increases up to 487nm for the comfort case, and to 574 for the handling one: In both cases the error will cause a digital error. We summarized sine test results in figures 18 and 19: The focus error

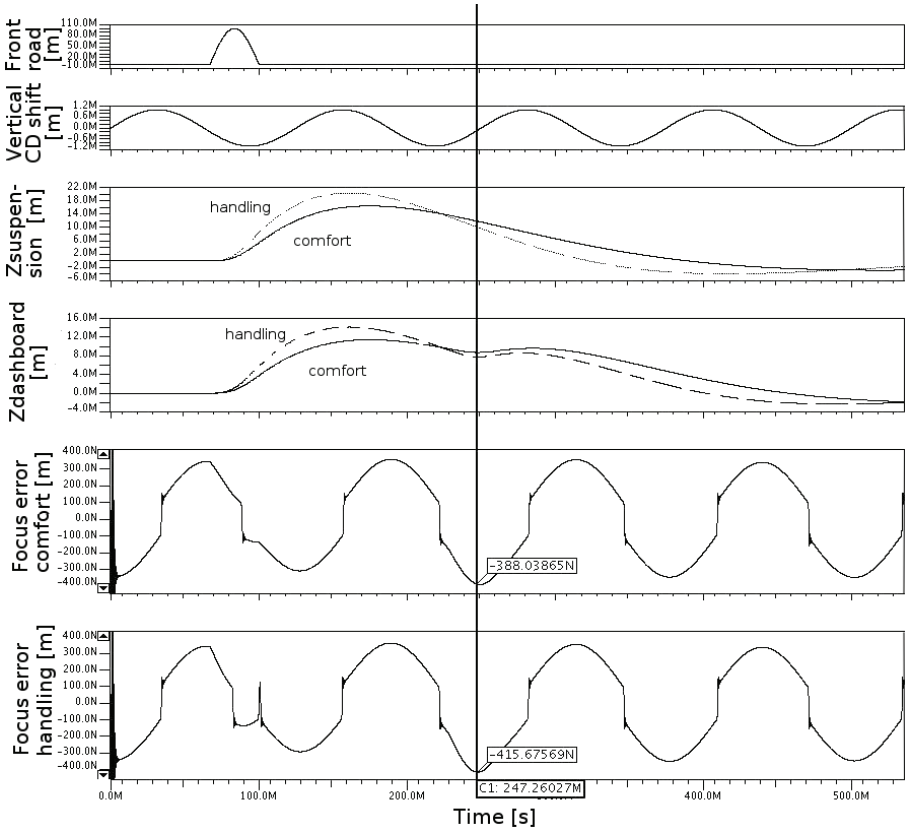

Fig. 16. Dashboard displacement and focus error in case of a bump road profile for a comfort and an handling vehicle suspension parameters. Disk vertical shift of 1mm peak and 8Hz frequency.

Test type	Bump ampl.	Δ T 33ms	Δ T 25ms	Δ T 20ms
Comfort vehicle model				
No CD misalign.	0.1m	207nm	207nm	206nm
	0.2m	314nm	313nm	213nm
CD misalign.	0.1m	390nm	351nm	356nm
	0.2m	439nm	358nm	370nm
Handling vehicle model				
CD mis.	0.1m	416nm	351nm	380nm

Table 3. Focus error caused by a bump road profile. CD misalignment has 1mm, 8Hz parameters.

is shown as a function of road profile frequency, which is swept within the values for which the two degrees of freedom model is valid for a 20cm and 10cm sine amplitude respectively. In figure 18 only a few tests (20Hz, 25Hz and 30Hz) reach the critical error range in case the

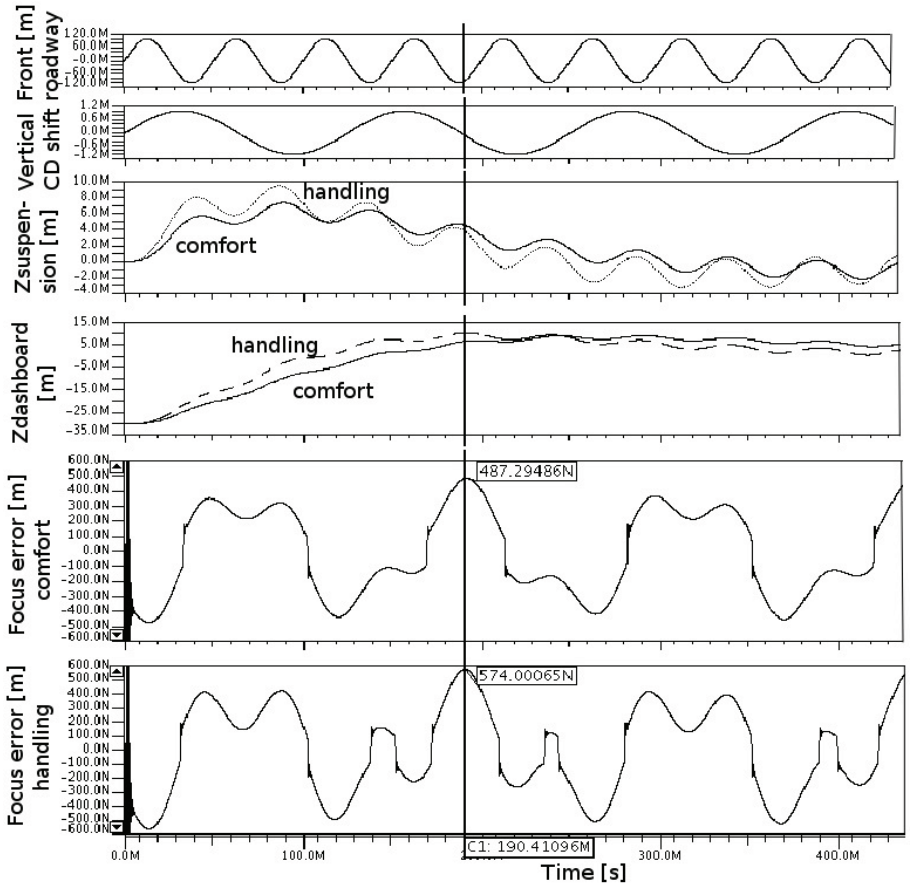

Fig. 17. CD player focus error for suspension parameters in the case of a comfort and a handling vehicle. The roadway profile is changing in a sinusoidal way in both the front and the back of the vehicle. Sine roadway profile (front an back): 0.1m peak, 25Hz. CD vertical shift max 1mm.

CD displacement is zero. On the other hand, the presence of the CD vertical shift causes an intolerable focusing error for almost every frequencies.
When a lower road irregularity peak is used (figure 19) then error is not critical when the disk has an ideal position. CD misalignment, instead, even in the comfort car model, produces an error around the limit range. The same tests conducted on a handling car bring the error above the limit, so that an audio mistake should be expected. This result supports the focus point of this work: The CD player manufacturer required the test to our partner as the car manufacturer received claims by customers of handling vehicles mounting those CD players on board. When tested by our partner by means of the traditional test equipment, they showed a worst behavior in the sine test as in our case. This has especially been verified when the CD players on the shaker plate was subject to vertical accelerations coherent with the dashboard of a handling vehicle. In every case reported in figure 18 and 19 a correlation

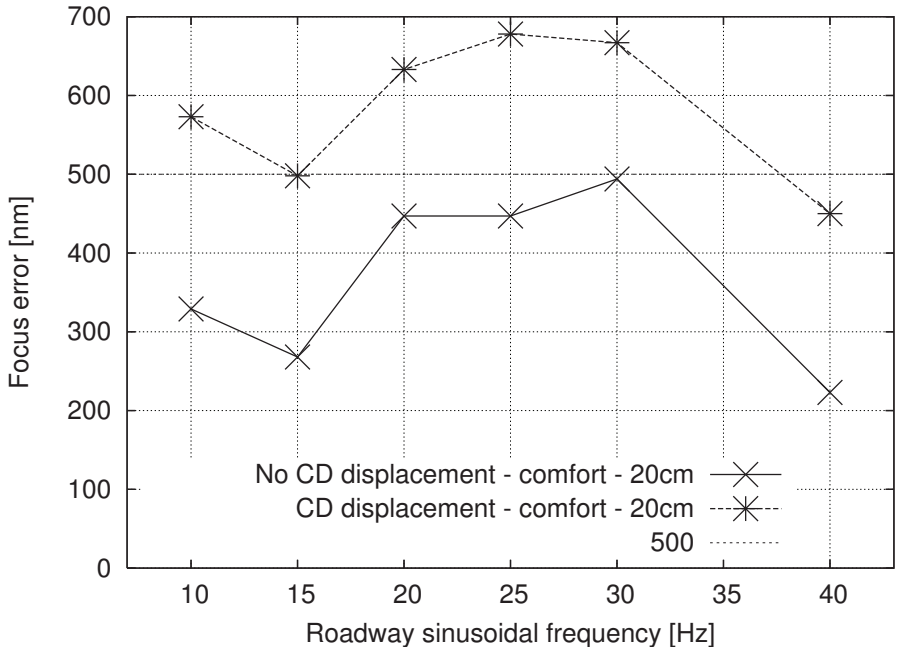

Fig. 18. Maximum focus error found with a sinusoidal roadway profile (0.2m peak) for different frequencies. No CD displacement effect, comfort vehicle parameters.

between road profile frequency and the mechanical car and CD player parameters can be observed, as only the values in the central range clearly show the worst behavior. It would be interesting to sweep such model parameters within proper ranges, once precisely provided by the manufacturers, as values adopted here are the only reliable ones we found. This way, a clean dependency between faults and electro-mechanical design choices could be pinpointed (e.g. CD mechanical structure rigidity and dumping parameters, coil properties, CD structure connection to the dashboard, amplification factors in the focusing differential amplifier and in the following power block,...), so that critical fault cases as the one we were involved in could be avoided. Anyway, the results achieved in this work show how this methodology may help both during fault and design analysis. The CD mechanical structure and pick-up electrical parameters, when chosen, are to be strictly related to the whole environment, especially to vehicle parameters and to real application conditions. Traditional test methodologies clearly do not take in consideration these aspects, if not in a late phase, as in the case of our industrial partners.

7. Conclusions

In this chapter we show how a VHDL-AMS multidisciplinary model can be used with success for setting up a new fault simulation methodology involving the automotive electro-mechanical system. We simulated a CD player electronical, optical and mechanical structure, its reaction to a vehicle dashboard-suspension-tyre shaking due to an irregular road profile. Results show good agreements with tests performed in laboratory. Furthermore,

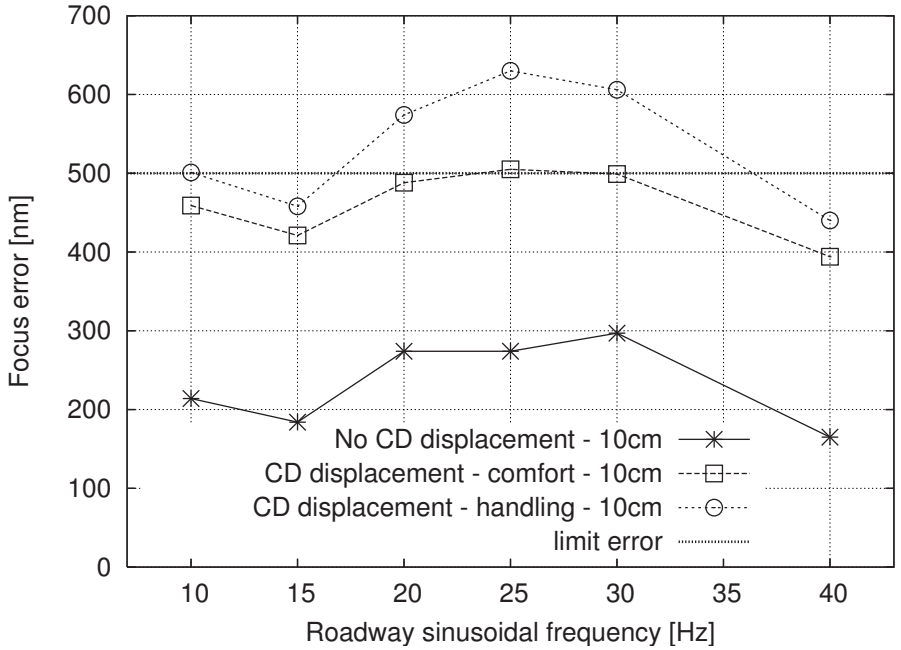

Fig. 19. Maximum focus error for a sinusoidal roadway profile (0.1m peak) for different frequencies. CD displacement effect, comfort and handling car parameters.

we demonstrate how fault cases could have been anticipated by both CD player and vehicle manufacturers still in the pre-production phase. This methodology allows thus to understand critical points of the system and to find possible solutions. For instance, pick-up electrical and mechanical parameters may be varied to more efficiently reaching the lens focus point on the CD audio track.

8. References

1076.1, I. S. (1999). *VHDL Analog and Mixed-Signal Extensions*, IEEE Std. 1076.1.

Bisoffi, A. (2006). *VHDL-AMS Modeling of a Vehicle CD-ROM system*, Politecnico di Torino, Thesis.

Christen, E. & Bakalar, K. (1999). Vhdl-ams–a hardware description language for analog and mixed-signal applications, *IEEE Transactions on Circuits and Systems—Part II: Analog and Digital Signal Processing* Vol. 46(No. 10): 1263–1272.

D. Metzner, G. P. & Schafer, J. (2002). Architecture development of mixed signal ics for automotive application with vhdl-ams, *Proceedings of IEEE International Behavioral Modeling and Simulation Conference (BMAS'02)*, San Josè, California.

E. Normark, L. Yang, C. W. & Nikitin, P. (n.d.). *Proceedings of IEEE International Behavioral Modeling and Simulation Conference (BMAS'04)*.

F. Gao, B. Blunier, A. M. & Moudni, A. E. (2010). A multiphysic dynamic 1-d model of a proton-exchange-membrane fuel-cell stack for real-time simulation, *IEEE TRANSACTIONS ON INDUSTRIAL ELECTRONICS* Vol.57(No. 6): 1853–1864.

F. Pecheux, C. L. & A.Vachoux (2005). Vhdl-ams and verilog-ams as alternative hardware description languages for efficient modeling of multidiscipline systems, *IEEE Transactions on Computer-Aided Design of Integrated Circuits and Systems* Vol. 24(No.2): 204–225.

Friedman, J. (2005). Matlab/simulink for automotive system design, *Proceedings of Design and Test Conference (DATE'05)*, Munich, Germany.

Godambe, N. J. & Shi, C.-J. R. (1998). Behavioral level noise modeling and jitter simulation of phase-locked loops with faults using vhdl-ams, *Journal of Electronic Testing Theory and Applications* Vol. 13(No. 1).

H. Boussetta, M. Marzencki, S. B. & Soudani, A. (2010). Efficient physical modeling of mems energy harvesting devices with vhdl-ams, *IEEE SENSORS JOURNAL* Vol. 10(No. 9): 1427 – 1437.

H. Casier, P. M. & Appeltans, K. (1998). Technology considerations for automotive, *Proceedings of IEEE International Design and Test Conference (DATE'98*, Paris, France.

J. Oudinot, S. Scotti, J. R. & Le-clerc, A. (2003). Full transceiver circuit simulation using vhdl-ams, *Journal of Microwave Engineering* pp. 29–33.

L.A.Barragan, D. Navarro, I. U. & Burdio, J. (2008). Fpga implementation of a switching frequency modulation circuit for emi reduction in resonant inverters for induction heating appliances, *IEEE TRANSACTIONS ON INDUSTRIAL ELECTRONICS* Vol. 55(No. 1): 11–20.

M. Gursoy, S. Jahn, B. D. & Pelz, G. (2008). Methodology to predict eme effects in can bus systems using vhdl-ams, *IEEE TRANSACTIONS ON ELECTROMAGNETIC COMPATIBILITY* Vol. 50(No. 4): 993–1002.

M. R. Casu, M. Graziano, M. C. & Zamboni, M. (2007). An effective ams top-down methodology applied to the design of a mixed-signal uwb system-on-chip, *Proceedings of IEEE Design Automation and Test Conference*, Nice, France.

Mansuripur, M. (1994). Principles of optical disk data storage, *Handbook of Optics* Vol. 1, Chapter 13.

MentorGraphics (2004). *ADVance MS (ADMS) Reference Manual*, Mentor Graphics.

Moser, E. & Mittwollen, N. (1998). Vhdl-ams: The missing link in system design - experiments with unified modelling in automotive engineering, *Proceedings of IEEE International Design and Test Conference (DATE'98)*, Paris, France.

M.R. Casu, M. C. & Graziano, M. (2008). A vhdl-ams simulation environment for an uwb impulse radio transceiver, *IEEE TRANSACTIONS ON CIRCUITS AND SYSTEMSI: REGULAR PAPERS,* Vol.55(No. 5): 1368 – 1381.

R. Ahola, D. W. & Sida, M. (2003). Bluetooth transceiver design with vhdl-ams.

Santarini, M. (2006). Design challenges steer automotive electronics, *EDN Magazine*.

V. Nguyen, P. L. & Naviner, J.-F. (2005). Vhdl-ams behavioral modelling and simulation of high-pass delta-sigma modulator, *Proceedings of IEEE International Behavioral Modeling and Simulation Conference (BMAS'05)*, San Josè, California.

W. Prodanov, M. V. & Buzas, R. (2009). A controller area network bus transceiver behavioral model for network design and simulation, *IEEE TRANSACTIONS ON INDUSTRIAL ELECTRONICS* Vol. 56(No. 9): 3762 – 3771.

W. Yang, H. C. & Yan, J. (2005). A high level vhdl-ams model design methodology for analog rf lna and mixer, *Proceedings of Int. Beh. Modeling and Simul. Conf. (BMAS'04)*, San Josè, California.

Wang, L. & Kazmierski, T. (2005a). Vhdl-ams based genetic optimization of a fuzzy

logic controller for automotive suspension system, *Proceedings of IEEE International Behavioral Modeling and Simulation Conference (BMAS'05)*, San Josè, California.

Wang, L. & Kazmierski, T. J. (2005b). Vhdl-ams modeling of an automotive vibration isolation seating system, *Proceedings of IASTED international conference on Signals and Systems (CSS 2005)*, Marina Del Rey, USA.